Applied Thermal Engineering 302 (2026) 131778

Contents lists available at ScienceDirect

Applied Thermal Engineering

journal homepage: www.elsevier.com/locate/apthermeng

Research Paper

Techno-economic and environmental assessment of hybrid propulsion systems based on solid oxide fuel cells for short-sea shipping

Paolo Marocco *, Gabriele Peyrani, Marta Gandiglio

Department of Energy, Politecnico di Torino, Corso Duca degli Abruzzi 24, 10129 Torino, Italy

ARTICLE INFO

Keywords:
SOFC
Fuel cells
Maritime decarbonisation
Hybrid propulsion systems
SOFC-ICE integration

ABSTRACT

Solid oxide fuel cells (SOFCs) are receiving increasing attention in the maritime sector as a decarbonisation option, owing to their high efficiency, fuel flexibility, and low pollutant emissions. This work investigates the retrofit of existing natural gas-fuelled vessels equipped with internal combustion engines (ICEs) through the integration of SOFC technology, using a short-sea RoPax ferry as a case study. A reference ICE-only configuration is compared with two SOFC-based hybrid layouts, including a fully integrated system exploiting anode off-gas recirculation. Detailed component models accounting for part-load operation are employed to perform a comprehensive assessment of energy performance, emissions, and economic feasibility. Sensitivity analyses on key parameters, including SOFC investment cost, fuel price, and vessel residual lifetime, are performed to identify the boundary conditions under which SOFC-ICE hybridisation becomes cost-effective.

The results show that SOFC integration significantly improves overall efficiency by mitigating inefficient ICE operation at partial loads. Compared to the ICE-only configuration, daily fuel consumption and CO_2 emissions are reduced by approximately 18%. Additional improvements from anode off-gas utilisation are observed but remain limited due to the relatively small SOFC-to-ICE size ratio imposed by the vessel operational profile. However, these benefits are expected to increase for vessel typologies characterised by higher baseload demand and longer sailing distances. From an environmental perspective, SOFC-powered harbour operation enables an almost complete abatement of NO_x and CO emissions (above 90%), highlighting the strong potential of SOFC systems to improve air quality in port areas. Finally, the economic analysis indicates that the vessel residual lifetime plays a key role in determining the viability of SOFC retrofitting. Under current assumptions, cost parity is approached for residual lifetimes above approximately 15 years. In addition, future reductions in SOFC investment costs and the introduction of carbon pricing are expected to further improve the economic attractiveness of the proposed solution. Overall, the results highlight SOFC-ICE hybridisation as an effective pathway to improve the efficiency and environmental performance of short-sea shipping.

1. Introduction

Maritime transport plays a central role in the global economy, as more than 80% of international trade is carried by sea [1]. At present, nearly all commercial vessels rely on internal combustion engines (ICEs) for propulsion, predominantly fuelled by heavy fuel oil and marine diesel oil, which results in substantial emissions of carbon dioxide (CO_2) and local air pollutants [2]. Overall, maritime shipping accounts for almost 3% of total global anthropogenic CO_2 emissions. Without effective mitigation measures, these emissions are expected to increase to levels 50–250% higher than today by 2050 due to continuous growth of international maritime commerce [3]. In response, the International Maritime Organization (IMO) has introduced increasingly stringent decarbonisation targets, aiming at a reduction of total GHG emissions of at least 20% by 2030 and 70% by 2040 compared to 2008 levels, with the ultimate objective of achieving net-zero emissions by 2050 [4]. In addition, regulatory drivers are increasingly affecting operational costs, as maritime transport has been included in the EU Emissions Trading

Abbreviations: AC, Alternating current; AOG, Anode-off gases; BoP, Balance of plant; CAPEX, Capital expenditures; DC, Direct current; ETS, Emissions trading system; HFO, Heavy fuel oil; ICE, Internal combustion engine; LHV, Lower heating value; MGO, Marine gas oil; NG, Natural gas; OPEX, Operating expenditures; RL, Residual lifetime; SI, Spark ignition; SOFC, Solid oxide fuel cell.

* Corresponding author.
E-mail address: paolo.marocco@polito.it (P. Marocco).

https://doi.org/10.1016/j.applthermaleng.2026.131778
Received 4 February 2026; Received in revised form 27 May 2026; Accepted 29 May 2026
Available online 6 June 2026
1359-4311/© 2026 The Authors. Published by Elsevier Ltd. This is an open access article under the CC BY-NC-ND license (http://creativecommons.org/licenses/by-nc-nd/4.0/).

System (EU ETS) since 1 January 2024 for ships ≥5000 gross tonnage, with a gradual phase-in of surrender obligations reaching full coverage by 2027 [5,6].

Meeting these ambitious targets requires a profound transformation of ship energy systems, relying on the combined adoption of low- and zero-carbon fuels and more efficient propulsion architectures. In this context, alternative fuels such as hydrogen, ammonia, methanol, and natural gas (NG) are being actively investigated, together with advanced powertrain solutions capable of reducing fuel consumption and emissions [7]. However, the suitability of each option strongly depends on vessel type, operational profile, technological maturity, and economic feasibility.

Battery-electric propulsion is receiving increasing attention in maritime applications, owing to its high efficiency and zero local emissions. However, the limited energy density of current battery technologies and the associated storage requirements restrict their applicability to short-range low-power coastal vessels, making them unsuitable as a stand-alone solution for deep-sea shipping [4].

Fuel cell technologies have also attracted growing interest in the maritime sector due to their ability to convert the chemical energy of fuels directly into electricity with higher efficiency and lower emissions than internal combustion engines [8]. The increasing number of pilot projects and research activities highlights their potential as a viable pathway for maritime decarbonisation, particularly when deployed within hybrid propulsion systems that enhance efficiency and operational flexibility [9]. Currently, the two main fuel cell technologies under investigation for transport applications are proton exchange membrane fuel cells (PEMFCs) and solid oxide fuel cells (SOFCs).

PEMFCs operate at low temperatures, typically below 80 °C, and are characterised by fast start-up, high power density, and excellent load-following capability [10]. Several modelling studies and demonstration projects have confirmed the technical feasibility of PEMFC-based systems onboard ships, often in combination with battery energy storage systems [11]. For instance, the MARANDA project developed and validated a hydrogen-fuelled PEMFC hybrid powertrain onboard a research vessel operating under Arctic-like marine conditions [12], while initiatives such as FLAGSHIPS and RH2IWER are currently deploying commercially operated hydrogen fuel cell vessels for inland and short-sea shipping applications [13,14]. However, PEMFCs require high-purity hydrogen as fuel and are highly sensitive to carbon monoxide poisoning, which complicates their integration with onboard fuel processing systems [2].

While PEMFCs represent the most mature and commercially available fuel cell technology, high-temperature fuel cell systems based on SOFCs are emerging as a promising option, due to their high conversion efficiency and capability to operate directly on a wide range of fuels. Recent review studies have highlighted the versatility of SOFC-based energy systems for stationary applications [15]. In addition, advanced system configurations and integration strategies have been extensively investigated to improve overall performance and flexibility [16]. SOFC technology has been increasingly explored for transport applications, including aviation [17–19], rail application [20,21], and the maritime sector [22,23]. In the maritime context, the integration of SOFC systems within combined cooling, heating, and power configurations has been investigated under dynamic operating conditions [24]. Furthermore, different integrated waste heat recovery systems based on SOFC technology have been investigated for combined power generation and refrigeration in ship applications [25]. According to De Graaf et al. [26], PEMFCs are more likely to prevail in short-distance applications, whereas SOFCs are expected to become the dominant technology for long-distance shipping owing to their broader fuel compatibility and higher system flexibility. Operating at temperatures above 700 °C, SOFCs offer several advantages over low-temperature systems, including higher electrical efficiency, intrinsic suitability for combined heat and power operation, and remarkable fuel flexibility [27]. SOFCs can operate directly on hydrocarbon fuels such as natural gas through internal or indirect reforming and are also compatible with future carbon-free fuels such as hydrogen and ammonia [28,29]. Their high operating temperature enables efficient waste heat recovery, which can be exploited for onboard heating services or to enhance system-level efficiency [30]. Field operation data from commercial-scale SOFC systems further confirm their high efficiency and environmental benefits at system level [31]. Despite these advantages, SOFCs also present important challenges. Their slow dynamic response and high thermal inertia limit their ability to follow rapid load variations, while frequent start-stop cycles may accelerate system degradation. Consequently, SOFCs are generally not well suited to operate as stand-alone prime movers in maritime applications and are more effectively deployed within hybrid power systems.

To address these limitations and enable flexible operation under highly dynamic marine power profiles, SOFCs are increasingly investigated within hybrid propulsion architectures. Hybridisation allows the SOFC to operate close to steady-state conditions, maximising efficiency and durability, while complementary power sources compensate for transient loads and peak demands. In this context, two main hybridisation pathways are typically considered: (i) SOFC-battery systems, where a battery energy storage system provides fast load-following capability and absorbs rapid power fluctuations, and (ii) SOFC-ICE systems, where an internal combustion engine supports peak propulsion power and ensures operational redundancy.

Recent studies on SOFC-battery hybrid propulsion have highlighted the importance of advanced energy management strategies to optimise efficiency and lifetime under dynamic conditions [32,33]. Similarly, SOFC-ICE hybridisation has been proposed as a pragmatic near-term solution, enabling substantial fuel savings while leveraging the high efficiency of fuel cells for baseload operation [34]. Integrated hybrid power systems combining SOFCs with marine engines and alternative fuels have further confirmed the fuel flexibility of SOFC-based solutions. For instance, methanol-fuelled SOFC-engine configurations have been evaluated, demonstrating excellent techno-economic performance and reduced carbon emissions [35]. In addition, hydrogen-based fuel blends have been explored within hybrid ship power systems, highlighting the adaptability of SOFC systems to different fuel compositions and operating conditions [36].

Different SOFC-ICE hybridisation strategies have been investigated in the literature. In non-integrated configurations, SOFCs and ICEs operate independently [37], whereas in more advanced integrated layouts, the chemical energy contained in the SOFC anode off-gases (AOG) is recovered by supplying these streams to the ICE, thereby reducing fuel consumption and improving overall system efficiency [38–40]. Elkafas et al. [38] performed an energy analysis and identified full-load SOFC operation combined with a 60% fuel utilisation factor as optimal design parameters for cruise operating conditions. Giap et al. [39] analysed two different SOFC-ICE hybridisation strategies from an energy and exergy perspective, reporting CO_2 emission reductions of 9% and 16% for indirect and direct coupling, respectively. Sapra et al. [40] identified a compromise solution achieving a 5.2% efficiency improvement and a 12% reduction in CO_2 compared to a conventional marine natural gas engine.

1.1. Aim and novelty of the present study

Within this context, the present work aims to provide a comprehensive assessment of SOFC-ICE hybrid propulsion systems for maritime applications, with a specific focus on the retrofitting of existing vessels. The study is conducted within the framework of the PRIN PNRR SOFFHICE project [41] and is based on a realistic case study of a short-sea RoPax ferry characterised by a representative operational profile for coastal shipping. In addition, the analysis is complemented by considerations on the applicability of the proposed approach to different vessel typologies and operating conditions.

Despite the growing number of studies on SOFC-based hybrid

propulsion systems, the analysis is often limited to specific aspects. In many cases, works focus either on energy performance or emission reduction, while integrated assessments considering energy, environmental and economic aspects together are still limited. However, such a combined evaluation is necessary to properly assess the feasibility of these systems in real maritime applications, particularly in retrofit scenarios where existing system constraints must be considered. In addition, although detailed electrochemical models of SOFC systems are frequently developed, their use at system level is not always supported by validation against experimental data or manufacturer-based performance data. At the same time, key operational constraints – such as minimum load limits, dynamic response and part-load behaviour – are often simplified. These aspects play a crucial role in determining system performance under realistic operating conditions.

The novelty of this work can be summarised as follows:

- An integrated assessment of energy performance, environmental impact, and economic implications is performed, with particular attention on pollutant emissions during both harbour operation and navigation. Additionally, different SOFC hybridisation strategies are analysed, including non-integrated and fully integrated SOFC-ICE configurations, allowing a direct comparison of their respective performance.
- A sensitivity analysis on key economic parameters, including fuel price, SOFC capital cost, and vessel residual lifetime, is carried out to identify the boundary conditions under which SOFC hybridisation becomes cost-effective, supporting the interpretation of results beyond case-specific assumptions.
- The accuracy and robustness of the analysis are enhanced through the adoption of part-load performance curves for both ICE and SOFC systems under variable operating conditions, as well as through the validation of the SOFC model against experimental data derived from long-term system operation.

By combining detailed component modelling with realistic vessel operating profiles, this study aims to derive useful insights for the application of SOFC-ICE hybrid propulsion systems in the maritime sector, supporting the transition towards more efficient and low-emission ship energy systems.

2. Case study

To assess the feasibility and performance of the proposed SOFC-ICE hybrid propulsion system, a real-world maritime application was selected as the reference case study. The analysis considers the Anna Mur, a RoPax ferry operating on short-sea routes in Italian territorial waters, which provides a representative operational profile for evaluating hybrid propulsion solutions in coastal shipping [38,42].

The vessel serves the route between Carloforte and Portovesme, connecting San Pietro Island to mainland Sardinia. It follows a fixed daily schedule, performing nine round trips between 05:00 and 23:00. Each voyage covers approximately 9.74 km and has a duration of about 30 min. The operational cycle is characterised by distinct load phases, including manoeuvring, navigation, and port hoteling. The daily power demand profile reflects these operational conditions. During navigation, propulsion power peaks at approximately 1190 kW, while hotel loads require a continuous demand of about 150 kW to supply onboard auxiliary systems during port stays. During nighttime mooring, when the vessel remains docked, the load is reduced to a minimum baseload of 75 kW, associated exclusively with hoteling services. The resulting daily power demand profile adopted for the simulations is shown in Fig. 1.

Natural gas was selected as the reference fuel within the SOFFHICE project based on technical feasibility, regulatory considerations, and alignment with the IMO 2030 emission reduction targets for maritime transport. The integration of NG-fuelled SOFC and ICE represents a pragmatic solution to improve overall system efficiency and reduce local pollutant emissions. Compared to conventional marine fuels such as heavy fuel oil (HFO) and marine gas oil (MGO), natural gas enables significant reductions in pollutant and CO_2 emissions, while remaining compatible with existing maritime fuel infrastructures. For these reasons, natural gas is considered an attractive transitional solution and a key enabler for the progressive adoption of future low- and zero-carbon fuels. In particular, the development of NG-based hybrid propulsion architectures is regarded as a stepping stone towards hydrogen- and ammonia-based solutions, both in terms of technological readiness and infrastructure deployment.

By demonstrating the feasibility of an NG-based SOFC-ICE hybrid configuration under realistic operating conditions, the SOFFHICE project aims to bridge the gap between current fossil-based propulsion systems and future zero-emission maritime solutions.

3. Methodology

3.1. Propulsion system configurations

In this analysis, three propulsion system configurations are explored (Fig. 2), all operating on natural gas:

1. ICE-only (Configuration C1)
2. Non-integrated SOFC-ICE system (Configuration C2)
3. Fully integrated SOFC-ICE with anode off-gas recirculation (Configuration C3)

The objective is to compare the performance of the three layouts and to assess the potential advantages of the hybrid SOFC-ICE approach.

Energy and environmental assessments are conducted to quantify total fuel consumption and CO_2 emissions, enabling a comparative evaluation of the configurations in terms of environmental impact over a representative daily operating cycle. In addition, pollutant emissions, specifically nitrogen oxides (NO_x) and carbon monoxide (CO), are estimated for all propulsion system layouts. Finally, a preliminary economic analysis is performed to identify the combinations of natural gas price

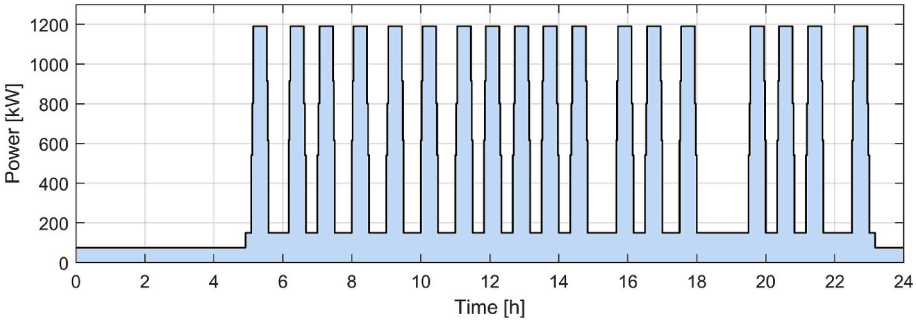


Fig. 1. Daily power profile of the selected RoPax vessel.

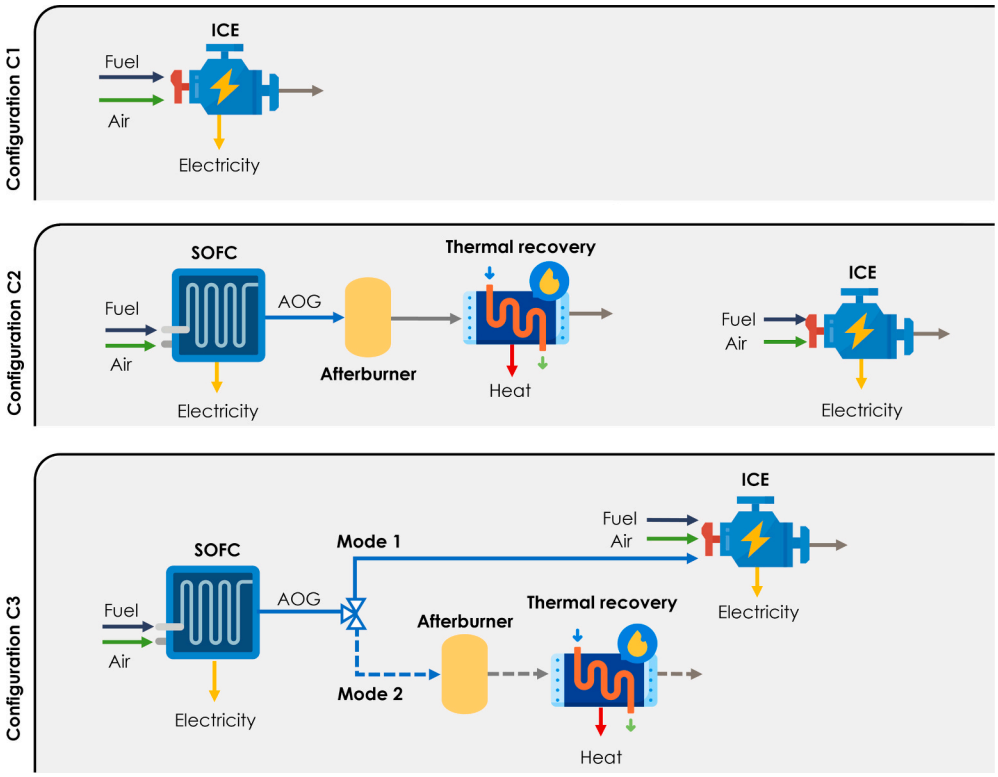


Fig. 2. Schematic representation of the propulsion system configurations considered in this study. In Configuration C3, the dashed arrows indicate the operating mode (Mode 2) when the ICE is shut down, i.e., when the vessel is at port and powered exclusively by the SOFC.

and SOFC investment cost under which the adoption of SOFC technology becomes the cost-optimal solution.

A simplified schematic representation of the layouts under analysis is shown in Fig. 2, while a more detailed process flow diagram, including the main system components, is provided in the Supplementary Material. The analysed system is based on a hybrid-electric architecture, in which both the ICE and the SOFC supply an onboard electrical network covering propulsion and hotel loads.

3.1.1. *ICE-only*

The first configuration represents the baseline scenario, in which the vessel relies exclusively on an internal combustion engine to meet the entire onboard power demand. The engine is rated at 1200 kW, allowing it to cover peak propulsion requirements. This configuration is adopted as the reference case against which the performance of the hybrid SOFC-ICE alternatives is assessed.

3.1.2. *Non-integrated SOFC-ICE system*

In the second configuration, a solid oxide fuel cell is introduced alongside the ICE, with the two systems operating independently. The SOFC is sized to cover the baseload power demand of 150 kW, which corresponds to the vessel's hoteling power requirements. To ensure flexibility and maintain high electrical efficiency, the SOFC is sized at 180 kW, allowing it to operate within its optimal efficiency range. The ICE, with a maximum rated power of 1200 kW, provides the remaining power to satisfy the propulsion demand.

One of the key advantages of the SOFC system is the potential for waste heat recovery from the exhaust gases. Owing to the high operating temperature of SOFCs (approximately 850 °C), the exhaust stream contains a significant amount of thermal energy that can be recovered to improve the overall system efficiency. As displayed in Fig. 2, the anode exhaust gases, which still contain unreacted fuel (whose amount depends on the selected fuel utilisation), are directed to an afterburner, where they undergo complete combustion. The resulting thermal energy is first used to preheat the SOFC inlet air and fuel streams, thereby reducing the need for additional fuel consumption. The remaining heat is then recovered through a dedicated thermal recovery unit and utilised for onboard heating applications, such as space heating and domestic hot water production.

Due to its high operating temperature and thermal inertia, the SOFC cannot respond rapidly to load variations compared to the ICE. To avoid thermal stress, maximum ramp-up and ramp-down rates of 1.8 and 3.0 kW/min are imposed, respectively [43]. During transient conditions, the ICE compensates for rapid load changes while the SOFC gradually adjusts to the new operating point, ensuring continuous power supply. In addition to ramp-rate constraints, the SOFC operating range is limited to 40–100% of its nominal power, in accordance with manufacturer specifications. Although part-load operation down to approximately 30% has been reported in the literature [44,45], very low-load conditions may not be thermally self-sustaining, potentially requiring additional balance-of-plant (BoP) support or external heating. Therefore, a minimum load of 40% was conservatively assumed in this study to ensure realistic and stable system operation.

Overall, the imposed ramp-rate limits and minimum load constraint are introduced to account, at a system level, for the thermal inertia and stability requirements of the SOFC and its BoP. Although thermal transients are not explicitly modelled, these constraints ensure operation within a realistic and thermally feasible regime.

3.1.3. *Fully integrated SOFC-ICE with anode off-gas recirculation*

In the third configuration, the SOFC and ICE are fully integrated, further enhancing system efficiency by exploiting the anode-off gases from the SOFC as an additional fuel source for the ICE.

During navigation (as displayed by Mode 1 in Fig. 2), when the ICE is in operation, the AOG (containing unreacted hydrogen and carbon monoxide) are supplied to the ICE instead of being directed to an afterburner. There, they contribute to the combustion process, thereby reducing the amount of natural gas required by the ICE. In this system

layout, the high-temperature SOFC exhaust gases are still used to preheat the SOFC inlet air and fuel streams, although without benefiting from the additional thermal energy that would be released by combustion in an afterburner.

The power management strategy remains unchanged with respect to configuration C2, with the SOFC supplying the baseload power and the ICE covering peak power requirements. Accordingly, the sizes of the main powertrain components are kept constant, with the SOFC rated at 180 kW and the ICE at 1200 kW. However, in Configuration C3, the ICE additionally benefits from the chemical energy contained in the SOFC unreacted fuel, resulting in fuel savings.

It should be noted that when the vessel is at port, only the SOFC is operated while the ICE is switched off. Under these conditions, the anode off-gases (instead of being supplied to the ICE) are directed to an afterburner to enable full thermal recovery, and the system operates analogously to Configuration C2, as indicated by Mode 2 in Fig. 2 (dashed arrows).

3.2. Component modelling

To analyse the hybrid propulsion system, accurate models of its main components are required. This section describes the modelling approach adopted for the ICE and the SOFC, focusing on their behaviour under varying load conditions. These models constitute the basis for assessing system operation and energy management across the different configurations.

3.2.1. ICE model

A spark-ignition (SI) engine fuelled with natural gas is adopted in this analysis. Among SI concepts, lean-burn operation is selected to enhance thermal efficiency and reduce NO_x emissions. Tavakoli et al. [46] investigated a maritime lean-burn SI engine operating under transient loads induced by wave-ship interactions, providing the basis for deriving the efficiency-load relationship adopted in this work. To ensure general applicability and account for differences in engine size, the ICE operating points are normalised with respect to the nominal engine power. The resulting efficiency curve, shown in Fig. 3, is used to evaluate the ICE fuel consumption over the operating day as a function of its operating point.

It should be noted that, when the ICE operates with AOG feeding from the SOFC (Mode 1 of Configuration C3), fuel savings are achieved, leading to an improvement over the reference performance shown in Fig. 3. The magnitude of this effect depends on the extent of AOG recirculation and the unreacted fuel content.

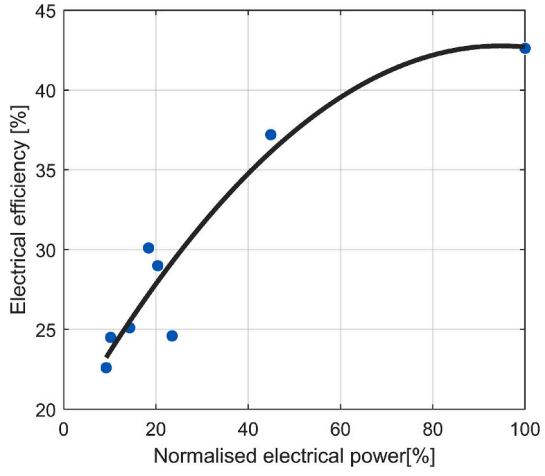


Fig. 3. ICE electrical efficiency curve as a function of the normalised electrical power.

3.2.2. SOFC model

To simulate SOFC performance under variable load conditions, a detailed electrochemical model of the SOFC cell is implemented, allowing voltage losses and their impact on power output to be explicitly accounted for. The modelling approach follows the methodology described in [47,48].

In SOFCs, both hydrogen (H_2) and carbon monoxide (CO) can be electrochemically oxidized at the anode. In this study, however, only hydrogen is assumed to participate in the electrochemical reaction, as its oxidation kinetics are reported to be approximately one order of magnitude faster than those of CO [49]. Under typical operating conditions, about 98% of the total current is attributed to H_2 oxidation, while the contribution of CO is negligible. This assumption simplifies the model without introducing significant inaccuracies [48].

The cell electrochemical model is developed to estimate the cell operating voltage (V_{OP}) starting from the open circuit voltage (V_{OCV}) and accounting for the irreversible losses occurring at both the anode and cathode, which depend on the operating current density (i). As shown in Eq. (1), these losses include activation (η_{act}), ohmic (η_{ohm}) and concentration (η_{conc}) contributions. The detailed methodology adopted to estimate V_{OP} is provided in the Supplementary Material.

$$V_{OP} = V_{OCV} - \eta_{act} - \eta_{ohm} - \eta_{conc} \tag{1}$$

Once the operating voltage is determined, the gross electrical power produced by a single cell in direct current (DC) at a given current density i can be calculated as shown in Eq. (2):

$$P_{SOFC,DC,cell} = V_{OP} \cdot i \cdot A_{cell} \tag{2}$$

where A_{cell} is the cell active area. In this work, the cell active area of an Elcogen SOFC cell [50], equal to 121 cm^2, is adopted as a reference.

The overall gross electrical power of the SOFC module is then obtained by multiplying the gross electrical power of a single cell by the total number of cells composing the module, denoted as n_{cell} and defined as follows:

$$n_{cell} = \frac{P_{SOFC,DC,nom}}{V_{OP,nom} \cdot i_{nom} \cdot A_{cell}} \tag{3}$$

where $P_{SOFC,DC,nom}$ is the nominal gross DC electrical power of the SOFC module, $V_{OP,nom}$ is the cell operating voltage under nominal conditions, and i_{nom} is the nominal current density. The nominal current density is assumed equal to 0.7 A/cm^2, in line with values commonly reported in the literature for high-temperature SOFCs.

The nominal gross DC electrical power of the SOFC module is expressed as:

$$P_{SOFC,DC,nom} = \frac{P_{SOFC,AC,nom} + P_{SOFC,AUX}}{\eta_{INV}} \tag{4}$$

where $P_{SOFC,AC,nom}$ is the net electrical power delivered in alternating current (AC) under nominal conditions, $P_{SOFC,AUX}$ is the electrical power consumed by SOFC system auxiliaries, and η_{INV} is the inverter efficiency.

The parameter $P_{SOFC,AC,nom}$ must be at least equal to the maximum electrical power required by the SOFC over the daily vessel load profile. As anticipated in Section 3.1, a value of 180 kW is assumed.

Auxiliary power consumption ($P_{SOFC,AUX}$) mainly includes the electrical power required to drive the inlet air and fuel blowers, which are needed to overcome pressure drops across the stack and balance-of-plant components. In this study, total pressure losses are assumed equal to 200 mbar for both the air and fuel streams. For the blowers, an isentropic efficiency of 0.8 and a mechanical efficiency of 0.9 are assumed.

The mass flow rates of the fuel ($\dot{m}_{fuel,SOFC}$) and air ($\dot{m}_{air,SOFC}$) streams at the SOFC module inlet are calculated according to Faraday's law. At a given operating point, the fuel mass flow rate, assuming 100% CH_4, is expressed as:

$$\dot{m}_{fuel,SOFC} = \frac{n_{cell} \cdot i \cdot A_{cell}}{8 \cdot F \cdot MW_{fuel} \cdot FU} \quad (5)$$

where F is the Faraday constant (96,485C/mol), MW_{fuel} is the fuel molecular weight, and FU is the fuel utilisation, which varies with the SOFC operating current density. In this study, fuel utilisation is assumed to converge to approximately 90% for operating powers above 60% of the nominal value, while it progressively decreases at lower loads (reaching about 70% at 40% of nominal power). This behaviour reflects real control strategies adopted in SOFC systems to ensure thermal self-sustainability at part load. At lower operating loads, the heat recovered from the electrochemical process is not sufficient to maintain the thermal balance of the system (including pre-reforming and inlet stream heating). Therefore, fuel utilisation is reduced to increase the energy content of the anode off-gas. While the exact parameterisation is specific to the adopted SOFC technology and cannot be fully disclosed for confidentiality reasons, the implemented trend is representative of typical SOFC operation.

Similarly, the air mass flow rate is calculated as:

$$\dot{m}_{air,SOFC} = \frac{n_{cell} \cdot i \cdot A_{cell}}{4 \cdot F \cdot y_{O2} \cdot \lambda_{air} \cdot MW_{air}} \quad (6)$$

where y_{O2} is the molar fraction of oxygen in air, λ_{air} is the air excess ratio, and MW_{air} is the molecular weight of air.

The air excess ratio is determined from the thermal balance of the SOFC system, aiming to remove the excess heat generated by the exothermic electrochemical reactions, net of the heat required for the endothermic reforming process. The remaining heat must be dissipated through the air flow ($\dot{m}_{air,SOFC}$) to maintain a stable SOFC operating temperature and limit thermal stresses. In Configuration C2 – and also in Configuration C3 when the ICE is not operating (Mode 2) – the exhaust streams from both the anode and cathode are directed to an afterburner, where the unreacted fuel in the anode exhaust is combusted. Since fuel utilisation in the SOFC is lower than 100%, this step allows the residual chemical energy to be converted into thermal energy, increasing the exhaust gas temperature. The high-temperature exhaust gases are then used to preheat the inlet fuel and air streams. A heat recovery unit is finally integrated into the system to extract the remaining thermal power from the exhaust gases, defined as $Q_{SOFC,rec}$.

The SOFC system performance is evaluated in terms of efficiency through two key indicators: net electrical efficiency ($\eta_{SOFC,el}$) and thermal efficiency ($\eta_{SOFC,th}$).

At a given operating point, the net electrical efficiency is defined as the ratio between the net AC electrical power delivered by the SOFC module (i.e., after accounting for auxiliary power consumption) and the chemical energy input, corresponding to the product of the fuel mass flow rate at the SOFC module inlet and its lower heating value (LHV_{fuel}):

$$\eta_{SOFC,el} = \frac{P_{SOFC,AC}}{\dot{m}_{fuel,SOFC} \cdot LHV_{fuel}} \quad (7)$$

where $P_{SOFC,AC}$ is the net AC electrical power of the SOFC module and $\dot{m}_{fuel,SOFC}$ is assessed according to Eq. (5).

Similarly, the thermal efficiency is expressed as the ratio between the recovered thermal power ($Q_{SOFC,rec}$) and the chemical energy input:

$$\eta_{SOFC,th} = \frac{Q_{SOFC,rec}}{\dot{m}_{fuel,SOFC} \cdot LHV_{fuel}} \quad (8)$$

where $Q_{SOFC,rec}$, as previously described, represents the thermal power recovered by the final heat recovery unit after preheating the inlet fuel and air streams.

Electrical and thermal efficiency curves are then developed by applying Eq. (7) and Eq. (8) while varying the SOFC current density up to its nominal value. In line with the ICE analysis (see Fig. 3), efficiency values are expressed as a function of the normalised operating power. Finally, the accuracy of the developed SOFC model is validated by comparing the simulated efficiency curves with experimental data available in the literature [31].

3.3. Energy and environmental analysis

An energy and environmental analysis is performed to assess the impact of the different propulsion system configurations in terms of fuel consumption (i.e., natural gas), CO_2 emissions, and pollutant emissions.

3.3.1. Fuel consumption estimation

Fuel consumption is evaluated based on the electrical efficiency curves of both the ICE (η_{ICE}) and the SOFC ($\eta_{SOFC,el}$). For a given time-dependent power demand, component efficiencies are determined at each time step as a function of their respective operating loads (P_{ICE} and $P_{SOFC,AC}$), enabling a realistic representation of part-load operation. The corresponding fuel mass flow rates of the ICE ($\dot{m}_{fuel,ICE}$) and SOFC ($\dot{m}_{fuel,SOFC}$) are then computed as:

$$\dot{m}_{fuel,ICE}(t) = \frac{P_{ICE}(t)}{\eta_{ICE}(t) \cdot LHV_{fuel}} \quad (9)$$

$$\dot{m}_{fuel,SOFC}(t) = \frac{P_{SOFC,AC}(t)}{\eta_{SOFC,el}(t) \cdot LHV_{fuel}} \quad (10)$$

Daily fuel consumption is obtained by integrating the fuel mass flow rates over a 24-h operating period.

In the ICE-only configuration (i.e., Configuration C1), total fuel consumption is exclusively associated with the ICE contribution. In the non-integrated SOFC-ICE configuration (i.e., Configuration C2), the SOFC operates independently supplying the baseload while the ICE covers load fluctuations, and the total fuel consumption is given by the sum of the individual ICE and SOFC contributions. In the fully integrated SOFC-ICE configuration (i.e., Configuration C3), the total fuel consumption again includes both ICE and SOFC contributions; however, during sailing conditions (Mode 1), the ICE fuel demand is further reduced by accounting for the additional energy contribution from the SOFC anode off-gases, which partially replace the direct natural gas input. In this case, the ICE fuel mass flow rate is updated as:

$$\dot{m}_{fuel,ICE}(t) = \frac{P_{ICE}(t)}{\eta_{ICE}(t) \cdot LHV_{fuel}} - \frac{P_{AOG}(t)}{LHV_{fuel}} \quad (11)$$

where P_{AOG} is the chemical power associated with the SOFC anode off-gases, and is defined as:

$$P_{AOG}(t) = LHV_{AOG} \cdot \dot{m}_{AOG}(t) \quad (12)$$

with $\dot{m}_{AOG}$ denoting the mass flow rate of the SOFC anode off-gases and LHV_{AOG} their lower heating value.

3.3.2. Emissions estimation

The emissions analysis quantifies the total production of CO_2, NO_x, and CO for the three investigated system configurations. Emissions are evaluated on a daily basis by combining fuel consumption data with emission factors derived from stoichiometric relations and experimental literature sources.

CO_2 emissions originate from methane oxidation in both the ICE and the SOFC. Although the underlying processes differ – combustion in the ICE and internal reforming followed by electrochemical oxidation in the SOFC – the overall carbon balance is equivalent. Assuming complete methane conversion, a constant mass-based emission factor (EF_{CO2}) of 2.75 kg of CO_2 per kg of CH_4 consumed is adopted to estimate total CO_2 emissions. Accordingly, the CO_2 mass flow rates from the ICE ($\dot{m}_{CO2,ICE}$) and SOFC ($\dot{m}_{CO2,SOFC}$) systems are expressed as:

$$\dot{m}_{CO2,ICE}(t) = EF_{CO2} \cdot \dot{m}_{fuel,ICE}(t) \quad (13)$$

$$\dot{m}_{CO2,SOFC}(t) = EF_{CO2} \cdot \dot{m}_{fuel,SOFC}(t) \quad (14)$$

Daily CO_2 emissions are then obtained by time integration of the corresponding mass flow rates.

The formation mechanisms of NO_x and CO differ significantly between the two technologies. In ICEs, NO_x is mainly produced through thermal mechanisms at high combustion temperatures, while CO originates from incomplete combustion. In contrast, SOFC stacks do not generate NO_x due to their electrochemical operating principle. However, limited NO_x and CO emissions may occur downstream when an afterburner is used to oxidise unreacted fuel species in the anode exhaust. To quantify these pollutants, emission factors expressed in mg/kWh are adopted from experimental literature sources [31,51]. These values represent the mass of each pollutant emitted per unit of electrical energy produced. At each time step, the resulting mass flow rates of NO_x and CO (denoted as pollutant j) from the ICE and SOFC are calculated as:

$$\dot{m}_{j,ICE}(t) = EF_j \cdot P_{ICE}(t) \quad (15)$$

$$\dot{m}_{j,SOFC}(t) = EF_j \cdot P_{SOFC,AC}(t) \quad (16)$$

Daily NO_x and CO emissions are subsequently obtained by integration over the operating period.

It should be noted that in Configuration 3 (fully integrated SOFC-ICE system), emissions strongly depend on the operating mode. During Mode 1, the afterburner (typically a major contributor to NO_x and CO formation in SOFC) is not used. As a result, SOFC-based NO_x emissions are effectively eliminated, since no high-temperature combustion occurs in the exhaust stream. Similarly, CO emissions from the SOFC are neglected, as the anode exhaust gas (containing residual CO) is directly supplied to the ICE and utilised as fuel. Consequently, under these conditions, the SOFC contributes exclusively to CO_2 emissions. Conversely, during Mode 2 (harbour operation with the ICE switched off), the SOFC contributes also to NO_x and CO emissions since the afterburner is activated to combust the anode exhaust gases.

The emission factors adopted for the ICE and SOFC systems, together with their literature sources, are summarised in Table 1.

A dedicated analysis is also performed to quantify pollutant emissions during harbour operation (i.e., hoteling load only), when the vessel is docked and auxiliary power demand must be continuously supplied. The evaluation of emissions is particularly relevant in the current regulatory context, where maritime transport is increasingly subject to decarbonisation policies. Recent developments include the extension of the EU ETS to shipping, covering emissions both during navigation and at berth [52], as well as the FuelEU Maritime Regulation, which promotes the adoption of low-emission and zero-emission solutions during port operations [53]. In addition, emissions monitoring frameworks such as the MRV Regulation [54] and IMO regulations targeting air pollutants in port areas [55] further highlight the importance of reducing emissions during harbour phases.

The harbour emissions assessment follows the same methodological approach adopted for the overall emissions analysis, with a specific focus on the hoteling period. To evaluate the benefits of SOFC integration, two scenarios are compared:

1. ICE-only hoteling, in which auxiliary power is supplied exclusively by the ICE
2. SOFC-powered hoteling, where the SOFC operates as the primary power source, with ICE operation limited to compensating for SOFC ramp-rate constraints.

Table 1
Emission factors of CO_2, NO_x, and CO for the ICE and the SOFC systems.

Emission factors	ICE	SOFC	Ref.
CO_2 emission factor, EF_{CO2} [kg_{CO2}/kg_{CH4}]	2.75	2.75	–
NO_x emission factor, EF_{NOx} [mg_{NOX}/kWh_{el}]	604.8	51.8	[31,51]
CO emission factor, EF_{CO} [mg_{CO}/kWh_{el}]	630	32.1	[31,51]

3.4. Economic analysis

The objective of the economic analysis is to assess the competitiveness of the different propulsion options from an economic standpoint in the context of the retrofitting of an existing vessel. The analysis is intended as a preliminary assessment, aimed at providing an initial indication of the techno-economic conditions (such as the SOFC investment cost, fuel price, and vessel residual lifetime) under which one configuration becomes preferable to another,

The net present cost (NPC) is adopted as the main economic indicator. Since the analysis refers to the retrofitting of an existing vessel, the NPC is evaluated over the remaining lifetime of the vessel rather than over the full lifetime of a newly built system. This includes the initial investment required for the retrofit and all future operating costs (namely operation and maintenance, component replacement, fuel expenditures, and CO_2-related costs) discounted over the residual lifetime.

The general formulation of the NPC is reported in Eq. (17), where j denotes the system components (with j referring to the ICE and the SOFC). The expression is adapted to each configuration under investigation; for instance, in Configuration C1, the contribution of the SOFC is not included.

$$C_{TOT} = \sum_j \left(C_{CAPEX,j}\right) + \sum_{n=1}^{RL} \frac{\sum_j \left(C_{OPEX,j}\right) + \sum_j \left(C_{REP,j}\right) + C_{fuel} + C_{CO_2}}{(1+d)^n} \quad (17)$$

where C_{TOT} is the total net present cost over the residual lifetime (RL) of the vessel, $C_{CAPEX,j}$ represents the capital expenditures (CAPEX) of the j-th component incurred at the beginning of the retrofit project (and therefore not discounted), $C_{OPEX,j}$ denotes the annual operating expenditures (OPEX) associated with the j-th component, computed as a fraction of its CAPEX; $C_{REP,j}$ is the replacement cost of the j-th component, incurred only in the years when replacement occurs and zero otherwise, C_{fuel} is the annual fuel cost, calculated as the product of the fuel price and the annual fuel consumption; C_{CO_2} is the annual cost associated with CO_2 emissions, based on the annual direct CO_2 emissions and the carbon price derived from the ETS market; and d is the discount rate.

In this analysis, the CAPEX associated with the ICE is assumed to be zero, as the study considers the retrofitting of an existing ICE-based propulsion system. The annual fuel consumption used to determine C_{fuel} is calculated by multiplying the daily fuel consumption – estimated according to the methodology described in Section 3.3.1 – by the number of operating days per year. Similarly, the annual direct CO_2 emissions required for the estimation of C_{CO_2} are derived from daily values (see Section 3.3.2).

It should be noted that, in the reference case, ETS-related costs are not included, as the vessel under investigation is currently not subject to the EU ETS scheme. However, an additional set of scenarios including CO_2 costs (assuming a current value of approximately 75 €/t_{CO2} [56]) is considered in order to assess the potential impact of future regulatory developments and carbon pricing policies on the economic competitiveness of the analysed configurations.

The main economic assumptions adopted as inputs for the economic analysis are summarised in Table 2. In particular, the SOFC CAPEX values (3000–5000 €/kW) are selected to reflect current market conditions, with higher values representative of early-stage or EU systems, and are further explored through sensitivity analysis due to their high uncertainty. The natural gas price is based on representative market values, while a wide range is considered to capture historical variability. Carbon pricing is included using ETS values consistent with recent market levels. The reference SOFC stack lifetime adopted in the baseline case (8 years) is assumed a priori as an input parameter for the techno-

Table 2
Main techno-economic assumptions.

	Value	Ref.
ICE		
Size	1200 kW (C1, C2 and C3)	
CAPEX	600 €/kW	[57]
OPEX (annual)	2% (% of CAPEX)	[57]
Lifetime	30 years	
SOFC		
System size	0 kW (C1); 180 kW (C2 and C3)	
System CAPEX	3000 and 5000 €/kW (reference) Sensitivity analysis: 1000–8000 €/kW	[57–60]
System OPEX (annual)	2% (% of CAPEX)	[57]
Stack replacement cost	45% (% of CAPEX)	[44]
Stack lifetime	8 years[a]	
Other assumptions		
Fuel price (natural gas)	30 €/MWh (reference) Sensitivity analysis: 10–150 €/MWh	[61]
Carbon price (ETS)	0 and 75 €/t_{CO2}	[56]
Discount rate	5%[a]	[57]
Vessel lifetime	30 years	[62,63]
Vessel residual lifetime (RL)	15 years (reference) Sensitivity analysis: 5 to 25 years	

[a] Sensitivity analyses on SOFC stack lifetime (4–10 years) and discount rate (2–11%) are reported in the Supplementary Material.

economic assessment and is further explored through sensitivity analysis in the Supplementary Material (from 4 to 10 years). Degradation effects are indirectly accounted for through the use of SOFC performance curves derived from long-term operation data of real systems, as well as through the sensitivity analysis on stack lifetime. However, a more detailed modelling of time-dependent SOFC and ICE degradation is beyond the scope of the present work and represents an aspect worth further investigation in future studies.

4. Results

4.1. SOFC and ICE performance analysis

4.1.1. SOFC efficiency

Before analysing the performance of the three propulsion system configurations, the developed SOFC model is validated by comparing its results with experimental data available in the literature. The validation is carried out using the net electrical efficiency curve. Fig. 4a shows the model predictions alongside reference literature data. The electrical efficiency curve exhibits a good agreement with experimental measurements, confirming that the model reliably reproduces the real-world performance of a solid oxide fuel cell module. Overall, the electrical efficiency initially increases with load, reaching a maximum value of approximately 60% at around 70% of the nominal AC electrical power, before slightly decreasing at full load. This behaviour reflects the trade-off between electrochemical performance and system losses. At low operating loads, the electrical efficiency is limited by reduced reactant utilisation. As the power output increases, fuel utilisation improves, leading to a peak in electrical efficiency. Beyond this optimal operating range, the progressive increase in ohmic and concentration losses results in a modest efficiency decline.

A comparison is also performed for thermal efficiency (Fig. 4b), which exhibits a wider spread in experimental values due to its strong dependence on the thermal recovery strategy adopted, which may vary according to end-user requirements. Despite this variability, the model predictions fall within the experimental range and accurately capture the overall trend of thermal efficiency as a function of the operating point, indicating consistency with real-world SOFC behaviour. Specifically, at low power levels, thermal efficiency remains relatively high, primarily as a result of low fuel utilisation. In this operating region, a significant fraction of the fuel is not directly consumed in the electrochemical reaction and remains available in the anode exhaust stream.

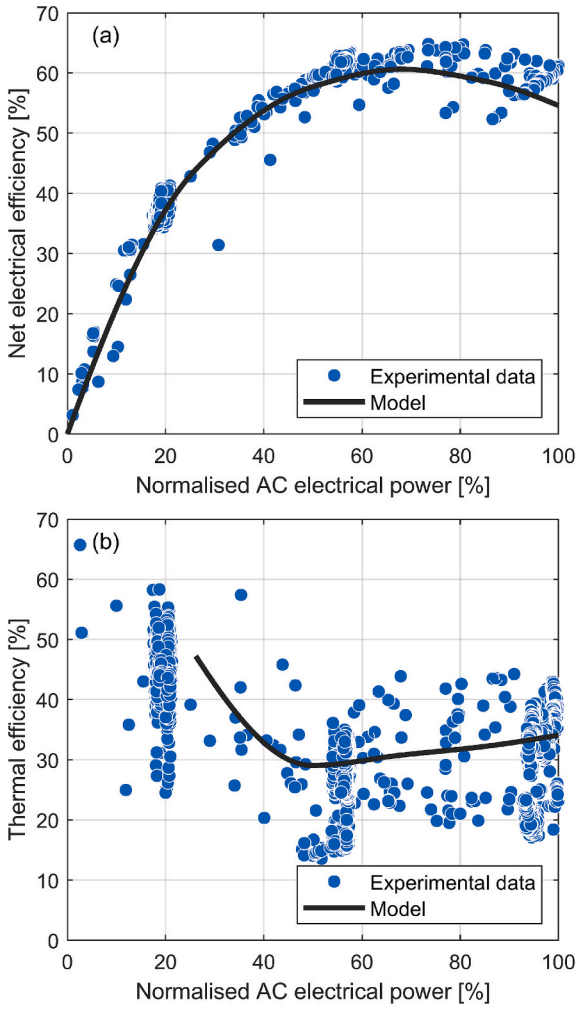


Fig. 4. SOFC net electrical (a) and thermal efficiency (b) curves as a function of the normalised electrical power. Experimental data are sourced from [31].

This unreacted fuel is typically combusted in an afterburner, increasing the amount of recoverable thermal energy and, consequently, the thermal efficiency. As the power output increases, fuel utilisation improves, reducing the fraction of unreacted fuel available for post-combustion and leading to a gradual decrease in thermal efficiency, which approaches approximately 30% at higher loads.

It should be noted that the thermal efficiency trend reported in Fig. 4b refers to a conventional configuration in which the anode off-gases are directed to an afterburner. In the case where the anode off-gases are instead supplied to the ICE (Mode 1 in Configuration C3), a markedly different thermal efficiency behaviour is expected, with lower values at partial loads. Under these conditions, the large fraction of unreacted fuel at low loads does not contribute to thermal energy production via post-combustion, but is instead exploited to enhance ICE performance.

Additional insights into SOFC operation under different load

Table 3
Anode off-gas properties at different load conditions. Results refer to an SOFC module of 180 kW.

SOFC current [%]	20	40	60	80	100
Normalised AC electrical power [%]	26.1	49.9	67.9	85.0	100
Anode exhaust flow rate [kg/h]	24.3	44.3	64.2	85.3	106.5
Anode exhaust LHV [MJ/kg]	9.35	4.19	2.06	1.88	1.81
Additional chemical power [kW]	63.0	51.6	36.8	44.5	53.6

conditions are provided in Table 3, which reports the AOG mass flow rate and lower heating value (LHV) for each operating point, considering an SOFC module of 180 kW. The last row of the table quantifies the resulting AOG chemical power, which could potentially be exploited by the ICE operating in Mode 1 of Configuration C3, thereby enhancing overall system efficiency through the recovery of unreacted fuel. At low SOFC loads (20% of the nominal current), the system operates with low fuel utilisation, resulting in a high fraction of unreacted fuel in the anode exhaust. Consequently, the anode off-gases exhibit a high lower heating value, leading to a significant potential contribution to ICE power output. However, under these conditions, the SOFC is unable to self-sustain the endothermic reforming reaction and would require an external heat source to ensure stable operation. In this analysis this problem is avoided by setting a minimum SOFC load of 40% of nominal power, which is in line with typical SOFC modulation ranges. As the SOFC load increases, fuel utilisation improves, progressively reducing the fraction of unreacted fuel in the anode outlet stream and, in turn, the additional chemical power available for the ICE. As shown in Table 3, the minimum AOG contribution to ICE power occurs at approximately 60–80% of the SOFC nominal load. At higher loads, the additional power slightly increases, as fuel utilisation approaches a plateau and no longer improves significantly.

Overall, while higher fuel utilisation enhances SOFC electrical efficiency, it simultaneously reduces the residual chemical energy available in the anode off-gases, thereby limiting its contribution to ICE power generation.

4.1.2. ICE efficiency

To provide a general overview of the potential effectiveness of AOG integration in ICE-based systems, Fig. 5 illustrates the variation of ICE electrical efficiency with respect to a reference operating curve, which is highlighted by the black dashed line. Three subplots are presented, corresponding to increasing values of the SOFC-to-ICE size ratio, ranging from 0.15 (current case study) up to 0.6. In each panel, ICE electrical efficiency is plotted as a function of ICE load (x-axis), while different coloured curves represent varying SOFC operating loads, from 40% to 100% of the nominal SOFC power.

Overall, the results clearly indicate the beneficial impact of AOG utilisation on ICE performance, as all coloured curves lie above the reference efficiency curve. At lower SOFC operating loads (around 40% of nominal power), the higher fraction of unreacted fuel in the anode off-gases results in a larger supplementary energy contribution to the ICE, leading to a more pronounced increase in electrical efficiency. However, it should be noted that operating the SOFC at low load is detrimental to its own electrical efficiency (see Fig. 4a), highlighting the importance of considering system-level trade-offs when evaluating hybrid SOFC-ICE configurations. The smallest ICE efficiency improvements are observed when the SOFC operates at approximately 60–80% of nominal power, consistently with the trends previously discussed in Table 3.

Furthermore, Fig. 5 shows that increasing the SOFC-to-ICE size ratio enhances ICE efficiency, as it allows a larger amount of AOG to be recovered and utilised by the ICE. In the present study, given the vessel load profile and the SOFC operational limits, the SOFC is sized to cover the baseload power demand, resulting in a relatively low size ratio of 0.15; consequently, the achievable enhancement in ICE efficiency through AOG utilisation remains limited. These findings suggest that alternative vessel operational profiles, characterised by more stable power demands and less pronounced load peaks than the one considered here (see Fig. 1), could benefit more substantially from full SOFC-ICE integration with anode off-gas recovery. This aspect is further explored in the Supplementary Material, where preliminary analyses based on additional case studies are presented to assess the influence of different load profiles and SOFC sizing strategies on system performance.

4.2. Energy analysis

In the ICE-only configuration (C1), the engine operates at low efficiency during nighttime operation and hoteling, when it runs under partial-load conditions, with efficiency decreasing to 21–24%. This confirms the poor performance of ICEs at low loads and highlights the potential benefits of hybridisation. During sailing, corresponding to peak power demand, the ICE operates at full load and reaches its maximum efficiency of approximately 43%. Over the entire day, the resulting average daily efficiency is about 37.7%.

In Configuration C2 (SOFC-ICE hybrid operation with independent units), the SOFC is sized to cover the hoteling load. Fig. 6 illustrates the power sharing between the SOFC and the ICE, with the SOFC contribution shown in red and the ICE contribution in grey; the dashed red line indicates the power output of the SOFC. During the initial load increase (around 05:00), the ICE compensates for the slow ramp-up of the SOFC. Conversely, at the end of the operational period (around 23:00), the delayed reduction of SOFC power results in a slight overproduction of electricity relative to the demand, which could theoretically be stored in an energy storage system or alternatively be curtailed. Overall, the hybrid configuration significantly improves system performance, particularly under low-load conditions, by mitigating inefficient ICE operation. The SOFC operates close to steady-state conditions, which are

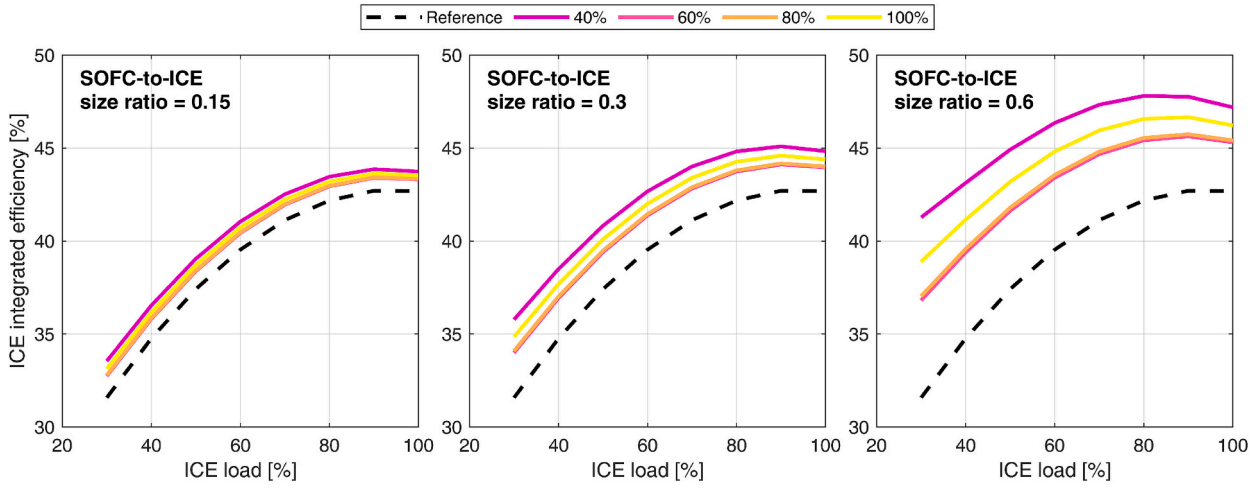


Fig. 5. ICE efficiency as a function of ICE load for different SOFC operating loads (40%–100% of nominal power). Three panels are shown with SOFC-to-ICE size ratios of 0.15, 0.3, and 0.6, respectively. The reference ICE efficiency curve is indicated by the black dashed line.

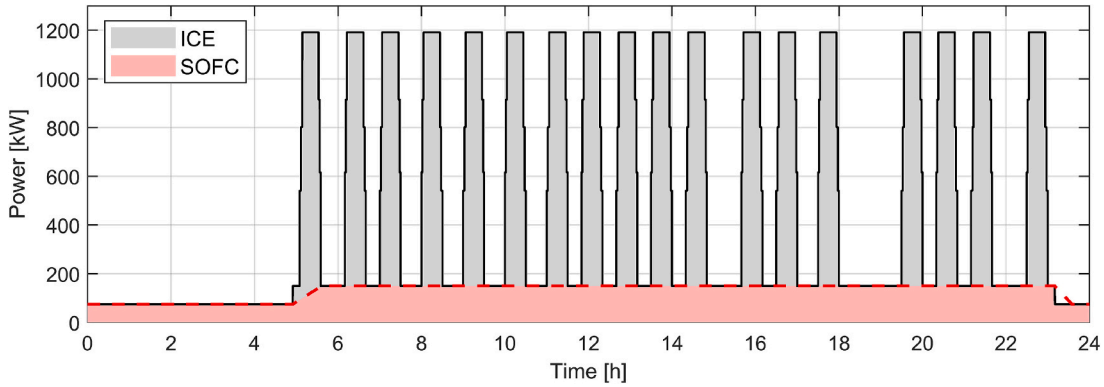


Fig. 6. Daily power distribution between the SOFC and ICE in the SOFC-based configurations (C2 and C3).

favourable for its performance, with efficiency remaining relatively stable in the range of 55–64% and an average daily value of 62.5%. As a result, the average daily efficiency of the hybrid propulsion system increases from 37.7% (Configuration C1) to approximately 45.9%.

Configuration C3 extends Configuration C2 by routing the SOFC anode-off gases to the ICE for additional energy recovery. Given the limited contribution of the SOFC to the total power demand, the beneficial effect of AOG utilisation is modest (as anticipated in Section 6.1), leading to an increase in the average daily efficiency of the hybrid system of approximately 1.6% compared to Configuration C2. The SOFC and ICE power profiles over the day remain unchanged with respect to Configuration C2 (see Fig. 6). The average daily efficiencies of the SOFC, ICE, and the overall hybrid system for all configurations are summarised in Table 4.

Overall, a 17.7% reduction in fuel consumption is achieved in Configuration C2 (1827 kg/day) relative to Configuration C1 (2220 kg/day), highlighting the efficiency benefits of the SOFC-ICE hybrid system. Configuration C3 provides a further, though more limited, improvement, with an additional 1.3% reduction in fuel consumption compared to Configuration C2. While the contribution of AOG utilisation is constrained by the relatively small share of SOFC power in the overall system, its integration still enables incremental fuel savings.

To further investigate the impact of SOFC sizing and operating conditions on system performance, additional analyses are presented in the Supplementary Material. In particular, scenarios with increased SOFC capacity combined with battery energy storage, as well as alternative vessel operating profiles, are considered. These analyses show that increasing the effective share of power supplied by the SOFC – through larger SOFC sizing and the integration of battery energy storage – enhances the potential benefits of system integration and anode off-gas utilisation. In addition, operating profiles characterised by longer navigation periods and more stable power demand, such as the tour ferry case, provide extended periods during which both the SOFC and ICE operate simultaneously, enabling more effective system integration and enhanced utilisation of the AOG stream.

Overall, the analysis confirms that the integration of an SOFC into the maritime power system yields substantial reductions in daily fuel consumption.

Table 4
Average daily electrical efficiencies of the SOFC, ICE, and the overall hybrid system in Configurations C1, C2, and C3.

Configuration	ICE	SOFC	Hybrid SOFC+ICE
C1	37.7%	–	37.7%
C2	41.7%	62.5%	45.9%
C3	42.6%	62.5%	46.6%

4.3. Environmental analysis

Based on the energy simulation results, CO_2 and pollutant (NO_x and CO) emissions are subsequently estimated. As illustrated in Fig. 7, the integration of the SOFC into the propulsion system leads to a substantial reduction in emissions. In the baseline Configuration C1, CO_2 emissions exceed 6 t per day, whereas SOFC hybridisation in Configuration C2 results in a 17.7% reduction in CO_2 emissions compared to the reference case. This reduction further increases to 19.0% in Configuration C3, as the additional utilisation of anode off-gases in the ICE lowers the overall fuel demand.

Owing to their electrochemical operation, SOFCs do not intrinsically generate NO_x emissions. Consequently, in Configuration C2, SOFC-related NO_x emissions arise solely from the combustion of unreacted fuel in the afterburner. In Configuration C3, during Mode 1 operation (when anode off-gases are directly supplied to the ICE), the afterburner is bypassed, resulting in the absence of pollutant formation. NO_x emissions only occur during Mode 2, when the vessel is at port; in this case, the ICE is shut down and the SOFC operates independently, with anode off-gases directed to the afterburner. Overall, NO_x emissions are reduced by 24.8% in Configuration C2 and by 25.8% in Configuration C3, where the limited use of the afterburner further suppresses NO_x formation. A similar behaviour is observed for CO emissions, which decrease by 25.8% in Configuration C2 and by 26.3% in Configuration C3.

A dedicated emissions analysis is finally performed for the harbour phase. This is particularly relevant in light of current regulations targeting emissions in port areas [55,64].

The results of the harbour emissions assessment (Fig. 8) show a marked reduction in CO_2, NO_x, and CO emissions when the SOFC is adopted as the primary power source in place of the ICE. In Configuration C1, where the ICE supplies the at-port auxiliary power demand, daily CO_2 emissions exceed 1500 kg. Transitioning to Configurations C2 and C3 – where the SOFC fully replaces the ICE during harbour operations – results in a 60% reduction in CO_2 emissions. This decrease is primarily attributed to the higher efficiency of the SOFC, which generates electricity through electrochemical conversion rather than combustion, thus reducing the overall natural gas consumption. The impact on NO_x emissions is even more pronounced: since ICEs are the main source of NO_x due to high-temperature combustion, eliminating ICE operation at port leads to a 91% reduction in NO_x emissions, with the residual contribution solely associated with afterburner operation. Similarly, CO emissions decrease by up to 94% in SOFC-based configurations compared to the ICE-only layout.

The near-complete abatement of pollutant emissions highlights the substantial air-quality benefits achievable through SOFC-based harbour power. These results underscore the potential of SOFC integration as an effective strategy to reduce the environmental footprint of ships while docked.

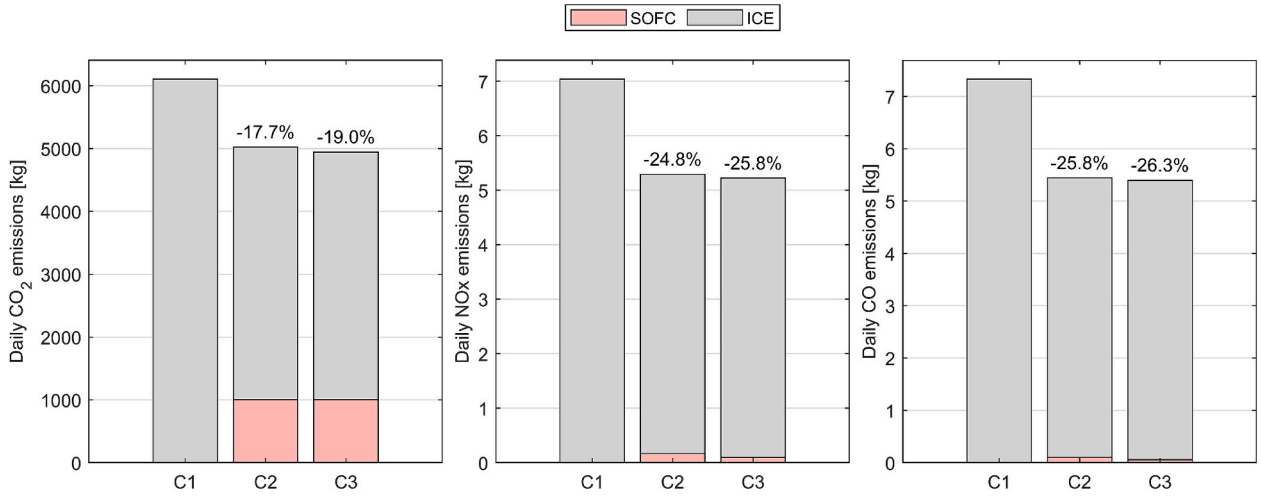


Fig. 7. Daily CO_2, NO_x and CO emissions (with the contribution of the SOFC and ICE) for Configurations C1, C2, and C3.

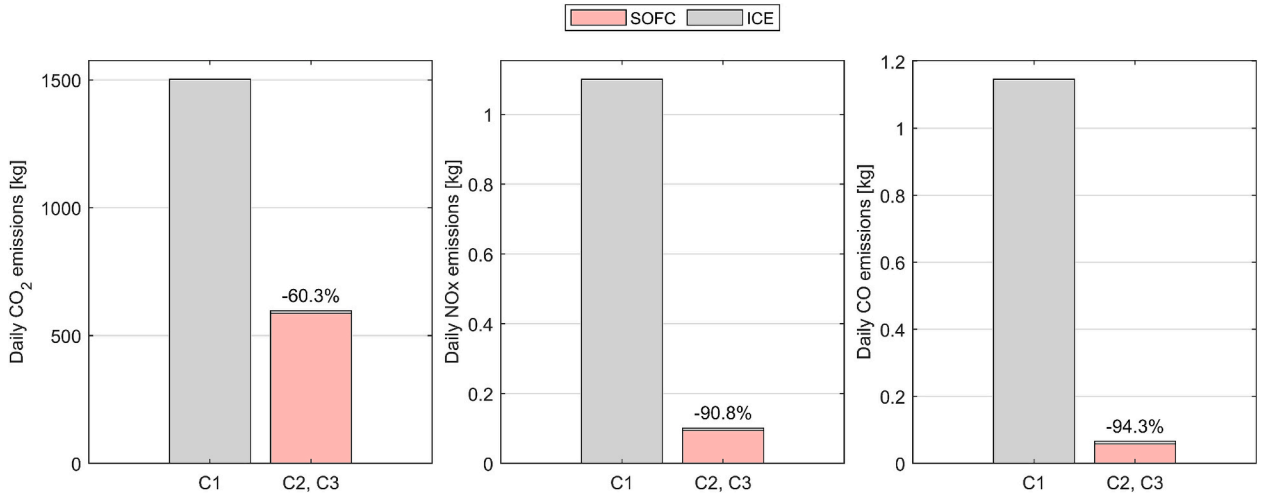


Fig. 8. Daily harbour CO_2, NO_x and CO emissions (with the contribution of the SOFC and ICE) for Configurations C1, C2, and C3.

4.4. Economic analysis

The economic analysis focuses on a comparative assessment between Configurations C1 and C2, with the primary objective of identifying the boundary conditions under which SOFC hybridisation represents the most cost-effective solution. Since, in the considered case study, the fuel consumption and CO_2 emissions of Configuration C3 are found to be quite comparable to those of Configuration C2, the general considerations reported below can also be extended to Configuration C3.

Results for the reference case are shown in Fig. 9, where the fuel price is set to 30 €/MWh and no ETS costs are considered. Given the current variability and uncertainty associated with SOFC capital expenditures, the analysis is performed assuming two representative values, namely 3000 and 5000 €/kW. Fig. 9a shows the NPC change of Configuration C2 relative to Configuration C1 as a function of the residual lifetime, varied between 5 and 25 years. The results clearly indicate that SOFC-based retrofitting is economically less attractive for short residual lifetimes, particularly below approximately 15 years. In this range, the additional investment cost of the SOFC system is not sufficiently compensated by fuel savings. As the residual lifetime increases, the NPC difference progressively decreases and tends to stabilise, indicating that longer operating periods allow for a more effective recovery of the initial investment. The SOFC CAPEX has a strong influence on the results. For instance, at a residual lifetime of 15 years, the NPC increase is approximately 20% when assuming a CAPEX of 5000 €/kW, whereas it decreases to about 5% for a CAPEX of 3000 €/kW. This suggests that SOFC-based retrofitting can already approach cost parity under favourable cost assumptions, considering that CAPEX values around 3000 €/kW are increasingly realistic, particularly in certain markets.

A detailed breakdown of the NPC is provided in Fig. 9b for a residual lifetime of 15 years. For a CAPEX of 3000 €/kW, the hybrid SOFC-ICE configuration exhibits only a slightly higher NPC compared to the ICE-only system, with a limited cost gap. The reduction in fuel consumption enabled by the SOFC almost compensates for the additional costs associated with the SOFC unit (including investment, operation and maintenance, and periodic module replacement). In contrast, for a CAPEX of 5000 €/kW, the economic disadvantage of the hybrid configuration becomes more pronounced, as the higher investment cost is no longer offset by fuel savings, leading to a noticeably higher overall NPC.

To better identify the SOFC CAPEX break-even level required for SOFC-based systems to become economically competitive, the SOFC investment cost is varied between 1000 and 8000 €/kW, with a step of 1000 €/kW. To provide a comprehensive assessment, a sensitivity analysis is also performed on the fuel price, which is varied between 10 and 150 €/MWh to reflect the range of natural gas prices observed in recent years. These sensitivities are carried out both without and with

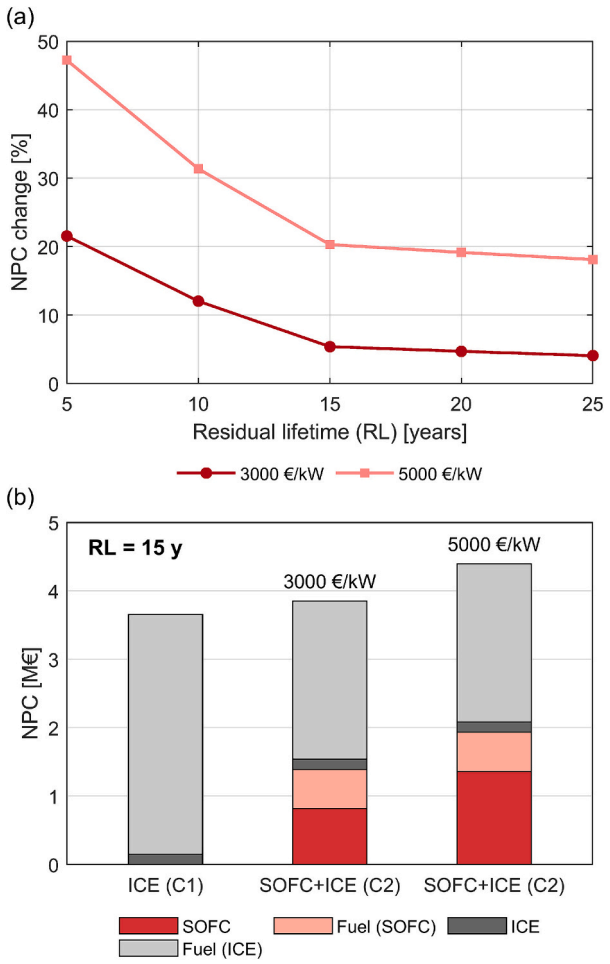


Fig. 9. (a) NPC change of Configuration C2 (SOFC-ICE) compared to Configuration C1 (ICE-only) as a function of the residual lifetime. (b) NPC of Configurations C1 and C2, including a breakdown of the different cost components, assuming a residual lifetime (RL) of 15 years. For both subplots, two SOFC CAPEX values of 3000 and 5000 €/kW are considered. ETS-related costs are not included.

the inclusion of ETS-related costs, assuming a carbon price of 75 €/t_{CO2} [56]. The results are presented in Fig. 10 in terms of the difference between the NPC of Configuration C2 and that of Configuration C1, considering a residual lifetime of 15 years (i.e., a vessel at mid-life). Negative values (red cells) indicate combinations of fuel price and SOFC CAPEX for which SOFC-based propulsion systems are more cost-effective, whereas positive values (grey cells) identify conditions under which ICE-only layouts are economically preferable.

As expected, SOFC hybridisation becomes increasingly attractive with decreasing SOFC CAPEX and under scenarios characterised by higher fuel prices. For current SOFC CAPEX values in the range of 3000–6000 €/kW, SOFC adoption becomes economically favourable when fuel prices exceed approximately 50–90 €/MWh (Fig. 10, left). A further improvement is observed when ETS-related costs are included, with the fuel price threshold reduced to approximately 30–70 €/MWh for SOFC-based configurations to become competitive (Fig. 10, right). From a market perspective, these break-even fuel price levels are consistent with the variability observed in recent years. Wholesale European natural gas prices (TTF) have typically ranged between approximately 25 and 65 €/MWh during 2025, while historical peaks above 100 €/MWh were recorded during periods of supply disruption and market volatility [61]. Therefore, the fuel price thresholds identified in this study fall within a realistic range for maritime applications, suggesting that SOFC hybridisation could become economically favourable under plausible near-term market conditions, particularly when carbon pricing is considered. Finally, considering the expected future SOFC CAPEX targets of 2000–3000 €/kW [65], SOFC hybridisation is projected to become a highly cost-effective option in the medium to long term.

The sensitivity analysis on both fuel price and SOFC CAPEX is then extended to different values of the vessel residual lifetime. Fig. 11 highlights the conditions under which SOFC-based retrofitting is economically attractive (red areas) and those for which the ICE-only configuration remains preferable (grey areas), as a function of natural gas price and SOFC CAPEX. As previously discussed, lower CAPEX values and higher natural gas prices favour the economic viability of the SOFC-based solution, as here indicated by the red region predominantly located in the upper-left portion of the plot. The residual lifetime of the vessel also plays a key role: increasing RL significantly improves the cost-effectiveness of SOFC retrofitting, as longer operating periods allow for a more effective amortisation of the initial investment. In particular, the economic advantage becomes evident for RL values above approximately 15 years, in agreement with the trends observed in Fig. 9a.

Additional sensitivity analyses on other parameters, including discount rate and SOFC stack lifetime, are reported in the Supplementary Material. In general, lower discount rates further enhance the attractiveness of SOFC retrofitting, as do longer SOFC lifetimes, due to reduced replacement costs over the project horizon.

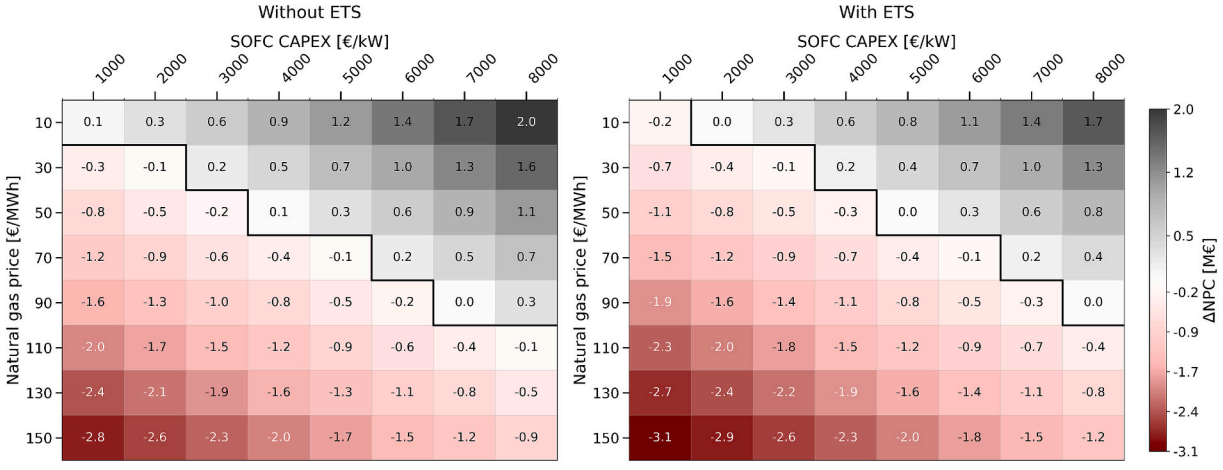


Fig. 10. Difference in NPC between Configuration C2 (SOFC + ICE) and Configuration C1 (ICE-only) as a function of fuel price (y-axis) and SOFC CAPEX (x-axis). Results are shown without and with ETS-related costs (ETS = 75 €/tCO_2). Residual lifetime is set to 15 years.

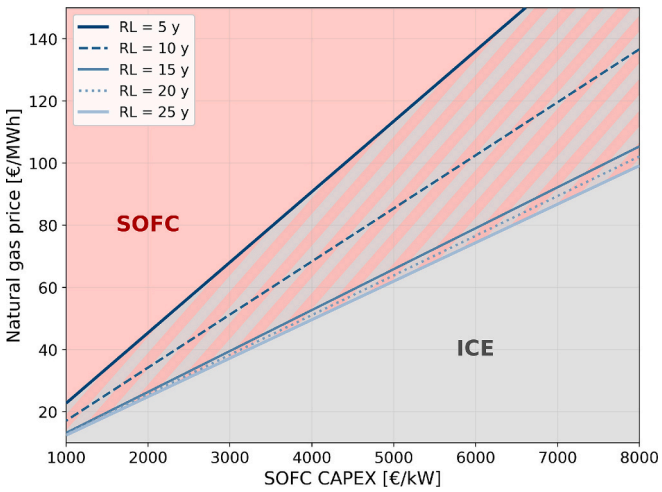


Fig. 11. Economic attractiveness of SOFC-based retrofitting as a function of natural gas price and SOFC CAPEX, for different values of vessel residual lifetime (RL). Red areas indicate conditions under which SOFC retrofitting is cost-effective (lower NPC), whereas grey areas correspond to scenarios where the ICE-only configuration is preferable. ETS-related costs are not included.

5. Conclusions

This work investigated the potential of SOFC hybridisation as an effective solution to improve the energy, environmental, and economic performance of maritime propulsion systems, with a specific focus on the retrofitting of existing vessels. A real-world case study of a short-sea RoPax ferry was analysed, comparing a conventional ICE-only configuration with two SOFC-ICE hybrid layouts, including a fully integrated system exploiting anode off-gas recirculation.

The results demonstrate that integrating an SOFC system to cover the baseload demand significantly enhances overall efficiency by mitigating inefficient ICE operation at partial loads. As a consequence, daily fuel consumption is reduced by approximately 18% compared to the reference ICE-only configuration, with a corresponding reduction in CO_2 emissions. The fully integrated SOFC-ICE configuration further improves performance by recovering the chemical energy of the SOFC anode off-gases within the ICE, although the additional benefit remains moderate due to the limited SOFC-to-ICE size ratio imposed by the vessel operational profile. Preliminary analyses suggest that higher SOFC contributions and more stable operating profiles, characterised by longer navigation periods, can significantly enhance the effectiveness of system integration and anode off-gas utilisation.

From an environmental perspective, SOFC hybridisation proves particularly effective in reducing pollutant emissions, especially during harbour operation. The replacement of ICE-based hoteling with SOFC-powered operation leads to an almost complete abatement (above 90%) of NO_x and CO emissions in port areas, highlighting the strong potential of SOFC systems to improve air quality in proximity to populated coastal regions.

The economic assessment highlights vessel residual lifetime as a key parameter for retrofit feasibility. Under current assumptions, SOFC-based retrofitting can approach cost parity with the ICE-only configuration, particularly for residual lifetimes above approximately 15 years. The economic attractiveness of the solution further increases under scenarios characterised by higher fuel prices, the inclusion of ETS-related costs, and expected medium- to long-term reductions in SOFC capital expenditure. In this respect, the progressive integration of maritime transport into the EU ETS framework and the realistic range of break-even natural gas prices strengthen the near-term economic potential of SOFC hybridisation. Sensitivity analyses also indicate that declining SOFC capital costs represent a key driver for future competitiveness, suggesting that SOFC-based hybrid systems may become a cost-effective option, especially for CAPEX values below approximately 3000–4000 €/kW.

Overall, the analysis confirms that SOFC-ICE hybrid propulsion offers an effective pathway towards maritime decarbonisation, combining improved efficiency, reduced emissions and promising economic prospects. Preliminary analyses already indicate that extending the proposed configurations to vessel typologies characterised by higher baseload demand and longer sailing distances can further enhance the benefits of SOFC integration. Future work will investigate these aspects in more detail, with particular focus on the impact of increased SOFC penetration and deeper system integration under different operational profiles.

CRediT authorship contribution statement

Paolo Marocco: Writing – review & editing, Writing – original draft, Visualization, Methodology, Investigation, Data curation, Conceptualization. **Gabriele Peyrani:** Writing – review & editing, Methodology, Investigation, Data curation, Conceptualization. **Marta Gandiglio:** Writing – review & editing, Visualization, Project administration, Methodology, Investigation, Data curation, Conceptualization.

Declaration of competing interest

The authors declare that they have no known competing financial interests or personal relationships that could have appeared to influence the work reported in this paper.

Acknowledgements

The Authors acknowledge the SOFFHICE (SOFC Hybridization with Internal Combustion Engine fuelled by Natural gas for maritime applications) Project, Prot. P2022K3TMP, funded by the European Union – NextGenerationEU, under the National Recovery and Resilience Plan (PNRR), Mission 4 Component 2 Investment 1.1 – National Program of Research (PNR) and Research Projects of Relevant National Interest (PRIN), Call for tender n. 1409 of 14-9-2022 of the University and Research Ministry (MUR). The work has been conducted in the framework of the AMPS (Automated Mass Production of SOC Stack) project (https://www.amps-project.eu/). The project is supported by the Clean Hydrogen Partnership and its members (GA: 101111882).

The authors acknowledge Lavinia Gaeta and Erica Bellomo for their contribution to the investigation of the energy and environmental benefits of SOFC-ICE integration, carried out as part of their master's thesis projects.

Appendix A. Supplementary data

Supplementary data to this article can be found online at https://doi.org/10.1016/j.applthermaleng.2026.131778.

Data availability

Data will be made available on request.

References

[1] UNCTAD, Review of Maritime Transport 2021. https://unctad.org/publication/review-maritime-transport-2021, 2021 (accessed January 7, 2026).
[2] M. Rivarolo, S. Piccardo, G.N. Montagna, D. Bellotti, A multi-criteria approach for comparing alternative fuels and energy systems onboard ships, Energy Convers. Manage.: X 20 (2023), https://doi.org/10.1016/j.ecmx.2023.100460.
[3] T.P.V. Zis, H.N. Psaraftis, F. Tillig, J.W. Ringsberg, Decarbonizing maritime transport: a Ro-Pax case study, Res. Transp. Bus. Manag. 37 (2020) 100565, https://doi.org/10.1016/J.RTBM.2020.100565.
[4] J.D. Ampah, A.A. Yusuf, S. Afrane, C. Jin, H. Liu, Reviewing two decades of cleaner alternative marine fuels: towards IMO'S decarbonization of the maritime transport sector, J. Clean. Prod. 320 (2021) 128871, https://doi.org/10.1016/J.JCLEPRO.2021.128871.

[5] DNV, EU ETS - Emissions Trading System. https://www.dnv.com/maritime/insights/topics/eu-emissions-trading-system/?utm_source=chatgpt.com, 2026 (accessed February 3, 2026).
[6] European Commission, Reducing Emissions from the Shipping Sector - Climate Action. https://climate.ec.europa.eu/eu-action/transport-decarbonisation/reducing-emissions-shipping-sector_en, 2023. (Accessed 3 February 2026).
[7] H. Xing, C. Stuart, S. Spence, H. Chen, Alternative fuel options for low carbon maritime transportation: pathways to 2050, J. Clean. Prod. 297 (2021) 126651, https://doi.org/10.1016/J.JCLEPRO.2021.126651.
[8] Z. Wang, B. Dong, Y. Wang, M. Li, H. Liu, F. Han, Analysis and evaluation of fuel cell technologies for sustainable ship power: energy efficiency and environmental impact, Energy Convers. Manage.: X 21 (2024) 100482, https://doi.org/10.1016/J.ECMX.2023.100482.
[9] Z. Fu, L. Lu, C. Zhang, Q. Xu, X. Zhang, Z. Gao, J. Li, Fuel cell and hydrogen in maritime application: a review on aspects of technology, cost and regulations, Sustain. Energy Techn. and Assess. 57 (2023) 103181, https://doi.org/10.1016/J.SETA.2023.103181.
[10] L. van Biert, M. Godjevac, K. Visser, P.V. Aravind, A review of fuel cell systems for maritime applications, J. Power Sources 327 (2016) 345–364, https://doi.org/10.1016/J.JPOWSOUR.2016.07.007.
[11] C. Dall'armi, D. Pivetta, R. Taccani, Health-conscious optimization of long-term operation for hybrid PEMFC ship propulsion systems, Energies 14 (2021) 3813, https://doi.org/10.3390/EN14133813.
[12] CORDIS - EU Research Results, Marine Application of a New Fuel Cell Powertrain Validated in Demanding Arctic Conditions (MARANDA), 2017, https://doi.org/10.3030/735717.
[13] CORDIS - EU Research Results, Clean Waterborne Transport in Europe (FLAGSHIPS), 2019, https://doi.org/10.3030/826215.
[14] CORDIS - EU Research Results, Renewable Hydrogen for Inland Waterway Emission Reduction (RH2IWER), 2023, https://doi.org/10.3030/101101358.
[15] O. Corigliano, L. Pagnotta, P. Fragiacomo, On the technology of Solid Oxide Fuel Cell (SOFC) energy systems for stationary power generation: a review, Sustainability 14 (2022) 15276, https://doi.org/10.3390/SU142215276.
[16] S. Mei, S. Wang, Y. Zhu, Y. Fan, X. Zhang, A review on system configurations and integration strategies of solid oxide fuel cell-based combined energy systems, Sustain. Energy Techn. and Assess. 88 (2026) 104933, https://doi.org/10.1016/J.SETA.2026.104933.
[17] G. Peyrani, P. Marocco, M. Gandiglio, R. Biga, M. Santarelli, Solid oxide fuel cells for aviation: a comparative evaluation against alternative propulsion technologies, ETransportation 24 (2025) 100408, https://doi.org/10.1016/j.etran.2025.100408.
[18] C. Li, K. Cheng, C. Li, X. Xiu, H. Liu, F. Guo, J. Qin, Performance analysis of multi turbines and SOFC combined power generation system for hypersonic vehicles, Appl. Therm. Eng. 257 (2024) 124461, https://doi.org/10.1016/J.APPLTHERMALENG.2024.124461.
[19] C. Li, K. Cheng, C. Li, X. Xiu, Z. Chen, J. Qin, Performance assessment of pressurized SOFC power generation system for hypersonic vehicles: thermodynamic analysis, system configuration optimization, Energy 315 (2025) 134377, https://doi.org/10.1016/J.ENERGY.2025.134377.
[20] Y. Zhang, J. Yu, N. Zhao, Z. Xu, Y. Yan, D. Wu, K. Blacktop, A. Tsolakis, Particle swarm optimization for a hybrid freight train powered by hydrogen or ammonia solid oxide fuel cells, Int. J. Hydrog. Energy 72 (2024) 626–641, https://doi.org/10.1016/J.IJHYDENE.2024.05.347.
[21] K.H.M. Al-Hamed, I. Dincer, A novel integrated solid-oxide fuel cell powering system for clean rail applications, Energy Convers. Manag. 205 (2020) 112327, https://doi.org/10.1016/J.ENCONMAN.2019.112327.
[22] P.A. Duong, Direct ammonia solid oxide fuel cells for marine application: status and perspectives, Renew. Sust. Energ. Rev. 235 (2026) 116968, https://doi.org/10.1016/J.RSER.2026.116968.
[23] S. Di Micco, V. Cigolotti, L. Mastropasqua, J. Brouwer, M. Minutillo, Ammonia-powered ships: concept design and feasibility assessment of powertrain systems for a sustainable approach in maritime industry, Energy Convers. Manage.: X 22 (2024) 100539, https://doi.org/10.1016/J.ECMX.2024.100539.
[24] X. Lu, W. Gang, S. Cai, Z. Tu, Advanced optimization framework for methane-fueled solid oxide fuel cell combined cooling heating and power system based on marine cyclic loads, Appl. Therm. Eng. 296 (2026) 130808, https://doi.org/10.1016/J.APPLTHERMALENG.2026.130808.
[25] W. Que, X. Li, X. Chen, M. Pan, C. Fu, L. Liang, T. Su, Potential of solid oxide fuel cells as marine engine assisted by combined cooling and power cogeneration systems, Appl. Therm. Eng. 254 (2024) 123821, https://doi.org/10.1016/J.APPLTHERMALENG.2024.123821.
[26] K.T. De Graaf, I.H.E. Hus, H.J. Van Leeuwen, G. Van de Kaa, Towards sustainable energy technologies in the maritime industry: the dominance battle for hydrogen fuel cell technology, Int. J. Hydrog. Energy 100 (2025) 156–162, https://doi.org/10.1016/J.IJHYDENE.2024.12.162.
[27] F. Baldi, S. Moret, K. Tammi, F. Maréchal, The role of solid oxide fuel cells in future ship energy systems, Energy 194 (2020) 116811, https://doi.org/10.1016/J.ENERGY.2019.116811.
[28] B.N. van Veldhuizen, L. van Biert, A. Amladi, T. Woudstra, K. Visser, P.V. Aravind, The effects of fuel type and cathode off-gas recirculation on combined heat and power generation of marine SOFC systems, Energy Convers. Manag. 276 (2023) 116498, https://doi.org/10.1016/j.enconman.2022.116498.
[29] E.A. Pina, B. van Veldhuizen, F. Marechal, J. Van Herle, A comparative techno-economic assessment of alternative fuels in SOFC systems for cruise ships, ECS Trans. 111 (2023) 2459–2472, https://doi.org/10.1149/11106.2459ecst.
[30] B.N. van Veldhuizen, L. van Biert, C. Ünlübayir, K. Visser, J.J. Hopman, P. V. Aravind, Component sizing and dynamic simulation of a low-emission power plant for cruise ships with solid oxide fuel cells, Energy Convers. Manag. 326 (2025) 119477, https://doi.org/10.1016/j.enconman.2024.119477.
[31] M. Gandiglio, P. Marocco, A. Nieminen, M. Santarelli, J. Kiviaho, Energy and environmental performance from field operation of commercial-scale SOFC systems, Int. J. Hydrog. Energy 85 (2024) 997–1009, https://doi.org/10.1016/j.ijhydene.2024.08.332.
[32] C. Ünlübayir, H. Youssfi, R.A. Khan, S.S. Ventura, D. Fortunati, J. Rinner, M. F. Börner, K.L. Quade, F. Ringbeck, D.U. Sauer, Comparative analysis and test bench validation of energy management methods for a hybrid marine propulsion system powered by batteries and solid oxide fuel cells, Appl. Energy 376 (2024) 124183, https://doi.org/10.1016/j.apenergy.2024.124183.
[33] CORDIS - EU Research Results, Nautical Integrated Hybrid Energy System for Long-Haul Cruise Ships (Nautilus), 2020, https://doi.org/10.3030/861647.
[34] Y. Feng, J. Qu, Y. Zhu, B. Wu, Y. Wu, Z. Xiao, J. Liu, Progress and prospect of the novel integrated SOFC-ICE hybrid power system: system design, mass and heat integration, system optimization and techno-economic analysis, Energy Convers. Manage.: X 18 (2023) 100350, https://doi.org/10.1016/J.ECMX.2023.100350.
[35] J. Qu, Y. Feng, Y. Zhu, B. Wu, Y. Wu, Z. Xiao, S. Zheng, Assessment of a methanol-fueled integrated hybrid power system of solid oxide fuel cell and low-speed two-stroke engine for maritime application, Appl. Therm. Eng. 230 (2023) 120735, https://doi.org/10.1016/J.APPLTHERMALENG.2023.120735.
[36] S. Seyam, I. Dincer, M. Agelin-Chaab, An innovative study on a hybridized ship powering system with fuel cells using hydrogen and clean fuel blends, Appl. Therm. Eng. 221 (2023) 119893, https://doi.org/10.1016/J.APPLTHERMALENG.2022.119893.
[37] A. Haseltalab, L. van Biert, H. Sapra, B. Mestemaker, R.R. Negenborn, Component sizing and energy management for SOFC-based ship power systems, Energy Convers. Manag. 245 (2021) 114625, https://doi.org/10.1016/J.ENCONMAN.2021.114625.
[38] A.G. Elkafas, L. Mantelli, S. Barberis, M. Rivarolo, Design performance analysis of a turbocharged solid oxide fuel cell integrated with internal combustion engine for maritime applications, Appl. Therm. Eng. 272 (2025) 126335, https://doi.org/10.1016/J.APPLTHERMALENG.2025.126335.
[39] V.T. Giap, Y.D. Lee, Y.S. Kim, K.Y. Ahn, D.H. Kim, J. Il Lee, System simulation and exergetic evaluation of hybrid propulsion system for crude oil tanker: a hybrid of solid-oxide fuel cell and gas engine, Energy Convers. Manag. 223 (2020) 113265, https://doi.org/10.1016/J.ENCONMAN.2020.113265.
[40] H. Sapra, J. Stam, J. Reurings, L. van Biert, W. van Sluijs, P. de Vos, K. Visser, A. P. Vellayani, H. Hopman, Integration of solid oxide fuel cell and internal combustion engine for maritime applications, Appl. Energy 281 (2021) 115854, https://doi.org/10.1016/J.APENERGY.2020.115854.
[41] PRIN PNRR National Italian Project, SOFC Hybridization with Internal Combustion Engine Fuelled by Natural Gas for Maritime Applications (SOFFHICE). https://www.linkedin.com/showcase/soffhice-project/, 2024. (Accessed 2 February 2026).
[42] A.G. Elkafas, M. Rivarolo, S. Barberis, A.F. Massardo, Techno-economic assessment of an advanced integration between sofc and ice onboard a short-distance ferry, in: 37th International Conference on Efficiency, Cost, Optimization, Simulation and Environmental Impact of Energy Systems 1, ECOS, 2024, pp. 204–215, https://doi.org/10.52202/077185-0018.
[43] CORDIS - EU Research Results, Commercial-Scale SOFC Systems (COMSOS), European Commission, 2018, https://doi.org/10.3030/779481.
[44] P. Marocco, M. Gandiglio, M. Santarelli, When SOFC-based cogeneration systems become convenient? A cost-optimal analysis, Energy Rep. 8 (2022) 8709–8721, https://doi.org/10.1016/j.egyr.2022.06.015.
[45] M. Gandiglio, A. Lanzini, M. Santarelli, M. Acri, T. Hakala, M. Rautanen, Results from an industrial size biogas-fed SOFC plant (the DEMOSOFC project), Int. J. Hydrog. Energy 45 (2020) 5449–5464, https://doi.org/10.1016/J.IJHYDENE.2019.08.022.
[46] S. Tavakoli, S. Saettone, S. Steen, P. Andersen, J. Schramm, E. Pedersen, Modeling and analysis of performance and emissions of marine lean-burn natural gas engine propulsion in waves, Appl. Energy 279 (2020) 115904, https://doi.org/10.1016/J.APENERGY.2020.115904.
[47] P. Pianko-Oprych, M. Palus, Simulation of SOFCs based power generation system using Aspen, Green Sci. 19 (2017) 8–15, https://doi.org/10.1515/pjct-2017-0061.
[48] M. Minutillo, A. Perna, E. Jannelli, SOFC and MCFC system level modeling for hybrid plants performance prediction, Int. J. Hydrog. Energy 39 (2014) 21688–21699, https://doi.org/10.1016/j.ijhydene.2014.09.082.
[49] A.V. Akkaya, Electrochemical model for performance analysis of a tubular SOFC, Int. J. Energy Res. 31 (2007) 79–98, https://doi.org/10.1002/er.1238.
[50] Elcogen, Elcogen Website – Solid Oxide Fuel Cells. 2026. https://elcogen.com/products. (Accessed 11 January 2026).
[51] P.G. Kristensen, J.K. Jensen, M. Nielsen, J.B. Illerup, Emission Factors for Gas Fired CHP Units < 25 MW, 2004.
[52] European Parliament and Council, Directive 2003/87/EC of the European Parliament and of the Council of 13 October 2003 Establishing a System for Greenhouse Gas Emission Allowance Trading Within the Union and Amending Council Directive 96/61/EC. https://eur-lex.europa.eu/legal-content/EN/TXT/?uri=CELEX%3A02003L0087-20240301, 2023 (accessed April 28, 2026).
[53] European Parliament and Council, Regulation (EU) 2023/1805 of the European Parliament and of the Council of 13 September 2023 on the Use of Renewable and Low-Carbon Fuels in Maritime Transport, and Amending Directive 2009/16/EC. https://eur-lex.europa.eu/legal-content/EN/TXT/?uri=CELEX%3A32023R1805, 2023 (accessed April 28, 2026).
[54] European Parliament and Council, Regulation (EU) 2015/757 of the European Parliament and of the Council of 29 April 2015 on the Monitoring, Reporting and

Verification of Greenhouse Gas Emissions from Maritime Transport, and Amending Directive 2009/16/EC. https://eur-lex.europa.eu/legal-content/EN/TXT/?uri=CELEX%3A02015R0757-20240101, 2015 (accessed April 28, 2026).
[55] IMO, New Sulphur Emission Limits Enter into Effect in the Mediterranean. https://www.imo.org/en/mediacentre/pages/whatsnew-2254.aspx, 2025 (accessed April 28, 2026).
[56] Trading Economics, EU Carbon Permits. https://tradingeconomics.com/commodity/carbon, 2026. (Accessed 21 April 2026).
[57] A.G. Elkafas, S. Barberis, D.T. Dong, A. Schönborn, M. Rivarolo, Multi-aspect assessment for the retrofitting of operating vessels in ports by using advanced power systems, Energy Convers. Manage.: X 26 (2025) 101011, https://doi.org/10.1016/J.ECMX.2025.101011.
[58] V. Cigolotti, M. Genovese, Stationary Fuel Cell Applications: Current and Future Technologies - Costs, Performances, and Potential. https://ieafuelcell.com/wp-content/uploads/2024/11/2021-stationary-application-performance.pdf, 2021. (Accessed 30 April 2026).
[59] Y.-H. Kiang, Solid Oxide Fuel Cell (SOFC) Module Pricing, Environment Energy Notes (EEN), 2025, https://doi.org/10.13140/RG.2.2.28825.74082 (accessed April 30, 2026).
[60] Clean Hydrogen Partnership, Strategic Research and Innovation Agenda 2021–2027, Brussels. https://www.clean-hydrogen.europa.eu/about-us/key-documents/strategic-research-and-innovation-agenda_en, 2022.
[61] Trading Economics, EU Natural Gas. https://tradingeconomics.com/commodity/eu-natural-gas, 2026. (Accessed 6 January 2026).
[62] J. Choi, K. Seo, S. Lim, Life cycle assessment for environment-friendly ferry service: a case study between South Korea and China, Reg. Stud. Mar. Sci. 89 (2025) 104297, https://doi.org/10.1016/J.RSMA.2025.104297.
[63] Discover Ferries, Sustainability. https://www.discoverferries.com/who-we-are/sustainability/?utm_source=chatgpt.com, 2024 (accessed April 30, 2026).
[64] European Commission, Reducing Emissions from the Shipping Sector. https://climate.ec.europa.eu/eu-action/transport-decarbonisation/reducing-emissions-shipping-sector_en#documentation, 2026.
[65] V. Cigolotti, M. Genovese, P. Fragiacomo, Comprehensive review on fuel cell technology for stationary applications as sustainable and efficient poly-generation energy systems, Energies 14 (2021) 4963, https://doi.org/10.3390/EN14164963.